

Gyrofluid vortex interaction

Alexander Kendl

*Institut für Ionenphysik und Angewandte Physik,
Universität Innsbruck, 6020 Innsbruck, Austria*

Abstract

Low-frequency turbulence in magnetised plasmas is intrinsically influenced by gyroscale effects across ion Larmor orbits. Here we show that fundamental vortex interactions like merging and co-advection in gyrofluid plasmas are essentially modified under the influence of gyroinduced vortex spiraling. For identical initial vorticity, the fate of co-rotating eddies is decided between accelerated merging or explosion by the asymmetry of initial density distributions. Structures in warm gyrofluid turbulence are characterised by gyrospinning enhanced filamentation into thin vorticity sheets.

I. INTRODUCTION

Vortices can be regarded as the basic constituents of turbulence. Vortex motion and interactions govern nonlinear structure formation, flow and convective transport properties in a variety of fluids. A particular case of interest are quasi-two-dimensional fluids, which are characterised by the possibility for formation of coherent structures and large scale (zonal) flows, a dual cascade, and the ideal conservation of enstrophy in addition to energy [1, 2]. Merging and filamentation of vortices are fundamental processes that underly these properties. Examples for quasi-2D fluids encompass stratified and rotating fluids, atmospheric and oceanic flows, or the cross-field dynamics of magnetised plasmas [3].

In magnetised space, laboratory or fusion plasmas, the fluidlike convection perpendicular to a magnetic field \mathbf{B} is governed by drifts, which describe the mean motion on top of fast charged particle gyration. In particular, the magnetic confinement of fusion plasmas is crucially determined through turbulent transport generated by drift-type instabilities, and their suppression by (turbulence driven) zonal or equilibrium flows [4, 5]. Turbulent convection in magnetised plasmas is dominated by the “E-cross-B” drift velocity $\mathbf{v}_E = \mathbf{E} \times \mathbf{B}/B^2$ in presence of a fluctuating electric field $\mathbf{E} = -\nabla\phi$. A localised electric potential $\phi(\mathbf{x}, t)$ leads to vortical E×B drift motion of the plasma around the potential perturbation. The vorticity $\boldsymbol{\Omega} = \nabla \times \mathbf{v}$ of E×B flows can be expressed as $\boldsymbol{\Omega} = (\mathbf{B}/B^2)\nabla_{\perp}^2\phi$ for constant \mathbf{B} . The electric potential ϕ thus has the role of a stream function for E×B flows.

Various instabilities driven by pressure gradients in magnetised plasmas typically result in drift vortex structures with sizes around the drift scale $\rho_0 = \sqrt{m_i T_e}/(eB)$, where m_i is the ion mass, T_e the electron temperature, and e the elementary charge. For warm ion plasmas with non-zero temperature ratio $\tau_i = T_i/T_e \sim 1$, the drift wave and vortex scales are in the order of $\rho_i = \sqrt{\tau_i} \rho_0$, the ion finite Larmor radius (FLR). Over the fast gyration of ions with particle charge $q_i = Ze$ around their gyrocenters (at cyclotron frequency $\omega_i = q_i B/m_i$) they effectively experience a ring-averaged electric potential ϕ_i rather than the potential at the gyrocenter (for low-frequency perturbations with $\omega \ll \omega_i$), and contribute to a quasi-neutral spatial distribution with approximately equal electron and ion particle densities $N_e(\mathbf{x}) \approx N_i(\mathbf{x})$ on average over the gyroorbit.

The framework for a description of magnetised plasmas governed by drift motion with FLR effects is efficiently given by gyrokinetic models evolving a 5D distribution function

in phase-space [6–8], or by gyrofluid models of appropriate respective fluid moments in 3D space [9–12]. In the following, the effects of finite Larmor orbits on fundamental vortex interactions are analysed within an isothermal gyrofluid model [13]. It is found that spiraling of vorticity induced by FLR effects in the presence of spatial asymmetry significantly alters the merger process and generates fine structured vorticity sheets. Specific initial conditions result either in strongly accelerated merging or in vortex explosion, with consequences for inverse turbulent cascade properties and zonal flows.

II. GYROFLUID MODEL FOR BASIC VORTEX INTERACTIONS

Here we employ a basic local (“delta-f”) gyrofluid model, derived from an energetically consistent gyrofluid electromagnetic model [14] in the limit of 2D isothermal dynamics in a straight and constant magnetic field. Details on the normalisation of the model equations and their numerical implementation can be found in Ref. [15]. Gyrofluid models do not dynamically evolve the particle densities $N_s(\mathbf{x}, t)$ of electrons and ions ($s \in e, i$), but rather their gyrocenter densities $n_s(\mathbf{x}, t)$. For small density fluctuation amplitudes both are connected through polarisation [10, 13, 16, 17] of gyroorbits by ϕ :

$$N_s = \Gamma_{1s} n_s + \frac{\mu_s}{\tau_s} (\Gamma_{0s} - 1) \phi. \quad (1)$$

The operator $\Gamma_{1s} = \Gamma_{0s}^{1/2}$ models gyroaveraging of the gyrocenter density, and Γ_{0s} reflects the gyroscreening of the potential ϕ in the mass dependent ($\mu_s \equiv m_s/m_i$) polarisation term. In wavenumber space $\Gamma_0(b_s) = I_0(b_s) \exp(-b_s)$ is expressed by the modified Bessel function I_0 with $b_s = \rho_s^2 k_\perp^2 = \tau_s \mu_s (\rho_0 k_\perp)^2$. For electrons, $\mu_e \ll 1$, and the gyro radius $\rho_e \ll \rho_i$ is negligible, so that $b_e \approx 0$ and $\Gamma_{0e} = \Gamma_{1e} \equiv 1$ can be assumed at ion gyro scales. The small electron mass also leads to negligible polarisation, so that particle and gyrocenter densities $N_e \approx n_e$ coincide. The electron and ion particle densities are connected by strict quasi-neutrality to $N_i \equiv N_e$ at scales much larger than the Debye length.

In the absence of driving, damping or parallel coupling the evolution equation for the gyrocenter densities in a homogeneous magnetic field then reflects incompressible mass conservation, and can (for normalised $B = 1$) in 2D be written as

$$\partial_t n_s + [\phi_s, n_s] = 0 \quad (2)$$

where the advection term $\mathbf{v}_E \cdot \nabla n$ is expressed in Poisson bracket notation by $[\phi, n] = (\partial_x \phi)(\partial_y n) - (\partial_y \phi)(\partial_x n)$, describing advection of electron density along contours of the potential ϕ , and of ion gyrocenter density along the gyroaveraged potential $\phi_i = \Gamma_{1i} \phi$. For numerical stability a hyperviscosity term $-\nu_4 \nabla^4 n_s$ is added to the right hand side of eq. (2).

The continuity eqs. (2) are closed by the quasi-neutrality condition $N_i = N_e$, which by the gyrodensity relation in eq. (1) gives the polarisation equation:

$$\frac{1}{\tau_i}(\Gamma_{0i} - 1)\phi = n_e - \Gamma_{1i}n_i. \quad (3)$$

The gyro-operators can be written in the Padé approximate forms $\Gamma_0 = [1 + b]^{-1}$ and $\Gamma_1 = [1 + (1/2)b]^{-1}$ and using $b_i = -\tau_i \mu_i (\rho_0 \nabla_\perp)^2$ in real space [10].

III. VORTEX MERGING FOR COLD IONS

In the cold ion limit $\tau_i = 0$ the polarisation equation reduces to $\nabla_\perp^2 \phi = n_e - n_i$, which for normalised $B = 1$ describes the deviation between electron and ion gyrocenter densities in relation to a scalar $\mathbf{E} \times \mathbf{B}$ vorticity $\Omega = \nabla_\perp^2 \phi$. Subtracting the ion from the electron gyrocenter density equation, eq. (2) in this cold limit transforms into the classical 2D Euler equation in vorticity representation:

$$d_t \Omega \equiv \partial_t \Omega + [\phi, \Omega] = 0 \quad (\text{for } \tau_i = 0). \quad (4)$$

Vortex interactions, in particular merging and co-advection, are in this limit akin to classical fluids, and the gyrocenter densities are just passively advected. For $\tau_i = 0$, a vortex that is defined by a localised spatial distribution $\Omega(\mathbf{x})$ can be initialised by any arbitrary initial density field $n_e(\mathbf{x})$ with an appropriate choice of $n_i(\mathbf{x}) \equiv n_e(\mathbf{x}) - \Omega(\mathbf{x})$: the further evolution of $\Omega(\mathbf{x}, t)$ in time through eq. (4) will not depend on the particular initial gyrocenter densities, but only on their difference.

In the following it is shown how finite ion temperature with $\tau_i > 0$ in magnetised plasmas leads to fundamentally different behaviour of the classical vortex merger and co-advection problems, and thus the resulting spectral properties of fully developed turbulence. In particular, the warm ion vortex merger problem intrinsically depends on the initial gyrocenter density distribution.

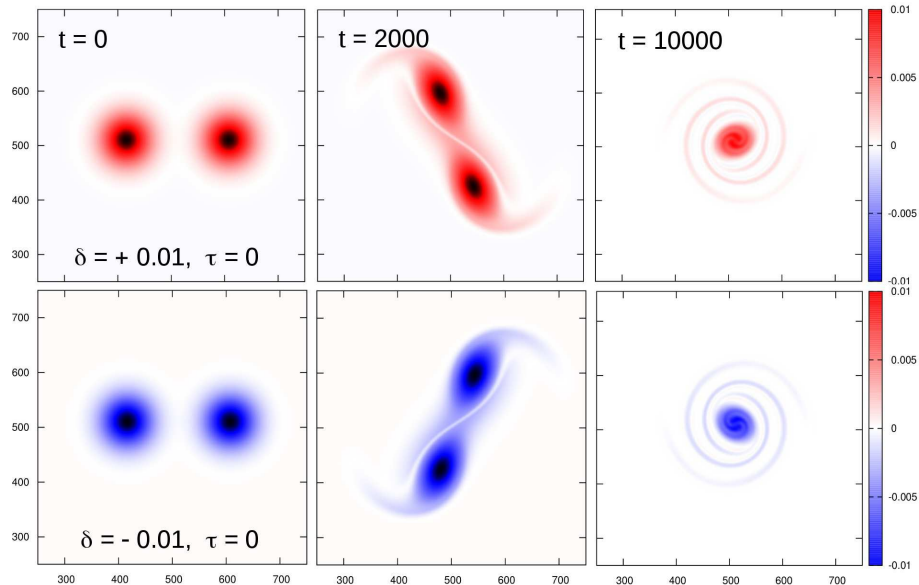


FIG. 1: Evolution of the vorticity $\Omega(\mathbf{x})$ field at several times during the co-rotating vortex pair interaction for $\tau_i = 0$: anti-symmetric with the sign of the vorticity amplitude δ (top/red: positive, bottom/blue: negative).

For comparability with classical fluid merger problems the vorticity is in the following initialised as a Gaussian $\Omega(\mathbf{x}, t_0) \sim \exp[-(\mathbf{x}/\sigma)^2]$ of width σ . In the gyrofluid model this may be obtained by a difference δ between the amplitude a of the electron compared to ion gyrocenter density, in the (x, y) plane perpendicular to \mathbf{B} :

$$n_{e0} = a \exp[-((x - x_0)/\sigma)^2 - ((y - y_0)/\sigma)^2], \quad (5)$$

$$n_{i0} = \Gamma_1^{-1}(1 - \delta \Gamma_0) n_{e0} \quad (6)$$

This initialises a vorticity $\Omega = \Gamma_0^{-1}(n_{e0} - \Gamma_1 n_{i0}) = \delta n_{e0}$ for both cold and warm plasmas. In the merger problem two vortices with the same amplitude are placed next to each other with an initial density peak distance Δ_0 .

The Euler equation as a standard model for fluid flow is, like the underlying Newtonian particle motions, invariant under parity transformation $\mathcal{P} : (t, \mathbf{x}, \mathbf{v}) \rightarrow (t, -\mathbf{x}, -\mathbf{v})$. The evolution of flow patterns is thus symmetric with respect to simultaneous point reflection ($\mathbf{x} \rightarrow -\mathbf{x}$) and reversal of the flow direction ($\mathbf{v} \rightarrow -\mathbf{v}$). This implies that also for the fluid-like (cold plasma) case $\tau_i = 0$ a change in sign of the initial (pseudovector) vorticity distribution ($\Omega(\mathbf{x}) \rightarrow -\Omega(\mathbf{x})$) leads to a spatially anti-symmetric evolution of the vortex merger.

For initialisation via eqs. (5, 6), this can either be obtained by $n_{e0} \rightarrow -n_{e0}$ (with amplitude $a \rightarrow -a$), or alternatively by leaving a positive but setting $\delta \rightarrow -\delta$.

In the cold fluid-like plasma case both choices have the same result: in Fig. 1 such a classical merging of co-rotating vortices is illustrated at several times for $\tau_i = 0$ with positive ($\delta = +0.01$, top) and negative ($\delta = -0.01$, bottom) initial vorticity. The vorticity field $\Omega(x, y, t)$ is shown in a $(62.5\rho_s)^2$ central section (corresponding to 500^2 grid points) of the $(128\rho_s)^2$ computational domain (1024^2 grid points). The initial vortex radius for this case is $\sigma = 6\rho_s$ with an initial peak separation $\Delta_0 = 4\sigma$. The evolution is a typical example for a 2D fluid vortex merger: vortices orbit each other by mutual advection and after a while (depending on initial separation) develop encircling vorticity and density veils, and coalesce on combined advection-diffusion time scales into a spiraling single vortex [18]. The ensembles with inverted initial vorticity evolve exactly anti-symmetrical: negative vorticity inverts the direction of co-rotation and of the final spiral arms of the merged vortex.

IV. FLR EFFECTS ON VORTEX MERGING

It had already been noted in the seminal work of Knorr et al. [9] from 1988 on theory of FLR effects in a guiding center plasma, that in a (reduced) exemplary simulation of vortex merging with and without FLR effects different behaviour appeared: while for zero Larmor radius the maxima remained separated, a coalescence had been observed for a finite Larmor radius [9].

In the following it is shown, that such FLR effects on vortex motion and vortex interactions in warm plasmas are generally a result of a breaking of the axial symmetry of the vortex in presence of any spatial asymmetry in the initial gyrocenter density distributions, which leads to FLR induced vortex spiraling.

However, for finite $\tau_i > 0$ no “generic” merger scenario like in the fluid case can be constructed: the temporal evolution of vorticity does not only depend on the initial (for example Gaussian) distribution $\Omega(\mathbf{x})$, but further on the specific gyrocenter initial density distributions $n_e(\mathbf{x})$ and $n_i(\mathbf{x})$ that generate this vorticity.

For warm plasmas the densities are not any more passively advected like in the cold case with $d_t\Omega = 0$ from eq. (4). The gyrofluid vorticity evolution can be understood more intuitively (compare Ref. [19]) in the long wave length limit ($b^2 \ll 1$) when the Padé form

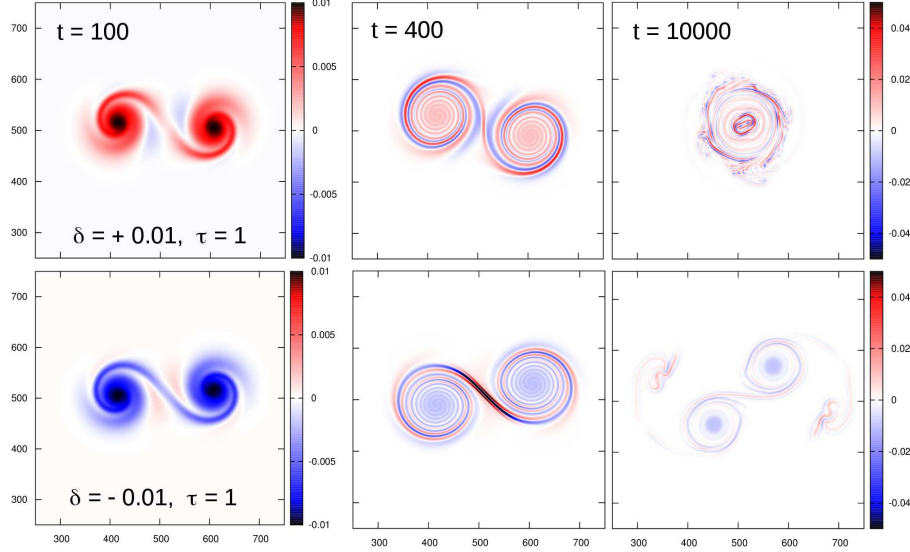


FIG. 2: $\Omega(\mathbf{x})$ during the co-rotating vortex pair interaction for $\tau_i = 1$. The sign of δ as the difference between initial electron and ion gyrocenter density amplitudes determines the fate of the pair towards merging or separation. ($t = 0$ as in Fig. 1.)

of the gyrooperators is Taylor approximated:

$$d_t \Omega \approx -\frac{\tau_i}{2} d_t \nabla_{\perp}^2 (n_e + \Omega) + \frac{\tau_i}{2} [\Omega, n_i] \quad (7)$$

$$\approx -\frac{\tau_i}{2} d_t \nabla_{\perp}^2 n_e + \frac{\tau_i}{2} [\Omega, n_e]. \quad (8)$$

In the first line terms up to order b^2 are kept, and in the second line up to b . For homogeneous \mathbf{B} , the identity $(\nabla_{\perp}^2 \mathbf{v}_E) \cdot \nabla_{\perp} n = [\Omega, n]$ has been used.

The first term on the right of eqs. (7, 8) contains the (gyroviscous cancelled) diamagnetic vorticity $\Omega_d = \nabla_{\perp}^2 p$ with $p = \tau_i n_e$, so that the generalised vorticity $W = \Omega + \frac{1}{2} \Omega_d$ obeys $d_t W \approx \frac{1}{2} [\Omega, p]$. This can be interpreted as an FLR induced contribution to polarisation by advection of vorticity along isobars of pressure p [19].

The Poisson bracket vanishes when the isocontours of axially symmetric density and vorticity profiles coincide. For a deviation from exact axial symmetry this term gives a significant contribution to the evolution of the (generalised) vorticity. The vortex dynamics for $\tau_i > 0$ thus depends on the specific initial values and momentary gradients of the gyrocenter densities.

Now the Gaussian merger is reconsidered for $\tau_i = 1$. Positive vorticity is initialised again by eqs. (5, 6) with $a = 1$ and $\delta = 0.01$ and otherwise same initial conditions as above. The

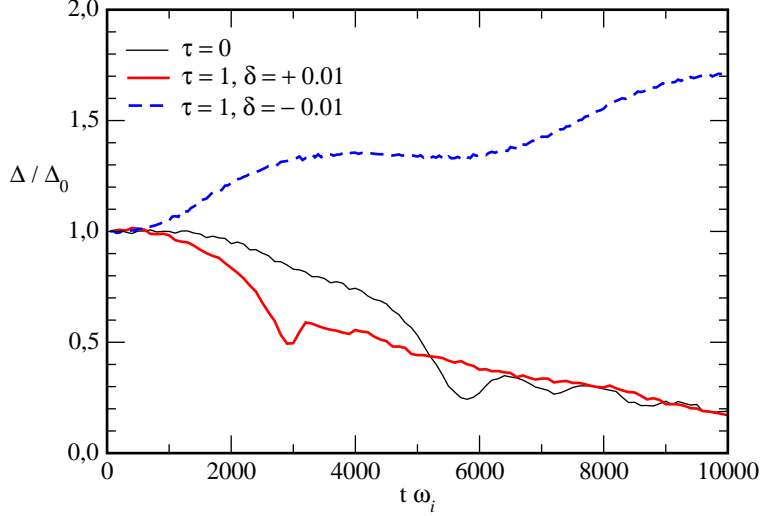


FIG. 3: *Relative vortex peak separation Δ/Δ_0 for initial distance $\Delta = 4\sigma$ with $\sigma = 6\rho_s$ for the classical fluid case ($\tau_i = 0$, thin black line) and the FLR cases with $\tau_i = 1$, and positive (bold red line) and negative (dashed blue line) initial vorticity relative to the magnetic field direction, respectively.*

evolution of $\Omega(\mathbf{x}, t)$ for this case is shown in Fig. 2 (top row) for various times. It is observed that already in the early stages of evolution ($t = 100 \omega_i^{-1}$) the vortices acquire spiral arms which rapidly spin up into a radial vorticity fine structure. The merging process is around twice as fast compared to the cold plasma case. The relative separation Δ/Δ_0 between peak densities of the vortices is plotted as a function of time in Fig. 3: The first minimum of distance for the warm merger is reached at around $t = 3000 \omega_i^{-1}$ (bold red curve) compared to the cold case at around $t = 6000 \omega_i^{-1}$ (thin black curve). For long times ($t > 8000 \omega_i^{-1}$) in the second diffusive stage the further merging appears (at least for the present numerical resolution and with $\nu_4 = 10^{-5}$) to occur on similar time scales as for the cold case.

The initialisation of negative vorticity is for $\tau_i > 0$ ambiguous. Negative initial density perturbation with $a = -1$ and $\delta = 0.01$ gives (similar to the cold cases of Fig. 1) an exact anti-symmetric vorticity evolution: the same pattern is obtained as on the top of Fig. 2, with simultaneous reversal of colours (sign of vorticity) and central point reflection. (This trivial reversed case is not explicitly shown in Fig. 2). Consequently the separation $\Delta(t)$ for $a = -1$ follows the same (bold red) curve as for $a = +1$ (with $\delta = +0.01$ for both) in Fig. 3.

The situation completely changes when the same initial $\Omega(\mathbf{x}, t_0)$ is obtained by keeping $a = +1$ but setting $\delta = -0.01$ and thus changing the relative local differences between

electron and ion gyrocenter densities. As can be seen by the second term on the right of eq. (7), n_i determines the FLR effect on polarisation. This means that at the positive Gaussian (quasi-neutral) density perturbation, the ion gyrocenters are not any more shifted outwards (as $n_i < n_e$ for $\delta > 0$) but inwards ($n_i > n_e$ for $\delta < 0$). This changes all gradients of n_i and thus the dynamical FLR contribution to polarisation.

The effect of this relative polarisation reversal by $(\delta > 0) \rightarrow (\delta < 0)$ on co-rotating vortices is significant: instead of a merger event, a vortex separation with increasing distance is obtained. This is illustrated as snapshots of vorticity in the bottom row of Fig. 2 and by the time evolution of the peak distances (blue dashed curve) in Fig. 3. Simulations for a range of initial separations $\Delta_0 = 2$ to 6 show the same general tendency, with expectedly faster merging for shorter separations.

V. DEPENDENCE OF VORTEX INTERACTIONS ON INITIAL CONDITIONS

It is not a priori clear which vorticity reversal method is physically more relevant. Vortices are in general not seeded, but appear dynamically mostly as a result of the specific effects of instabilities on electron and ion densities. An important mechanism for vorticity generation is the drift wave instability, driven by a nonadiabatic parallel electron response in the presence of a cross-field density gradient [4]. For low collisionality the relation between electron density and potential can however often be regarded as nearly adiabatic, following approximately a Boltzmann relation with $n_e \sim \phi$.

We can also construct a vortex merger problem for such “adiabatic” vortices. The constraint $n_e(\mathbf{x}, t_0) \equiv \phi(\mathbf{x}, t_0)$ implies that initially $\Omega = \nabla_{\perp}^2 \phi = \nabla_{\perp}^2 n_e \sim \Omega_{d/2}$. In particular, setting $\phi = n_e$ in eq. (3) for a given $\phi(\mathbf{x}, t_0)$ initialises $n_i \equiv \Gamma_1^{-1} [1 + \frac{1}{\tau_i} (1 - \Gamma_0)] \phi$, which is readily evaluated in wave number space. The choice is now whether to initialise Gaussian density/potential “adiabatic blobs” (which yields a shielded vorticity), or “adiabatic Gaussian” vorticities. The latter can be achieved by inversion of a defined (Gaussian) $\Omega(\mathbf{x}, t_0)$ to $\phi = n_e = \nabla_{\perp}^{-2} \Omega$.

The “adiabatic blobs” case first develops small satellite vortices which are sheared off through the shielding reversed vorticity rings around the centers. Subsequent collision of the satellites between the vortices rapidly results in an explosive repulsion after formation of a vorticity tangle. The situation is depicted in Fig. 4.

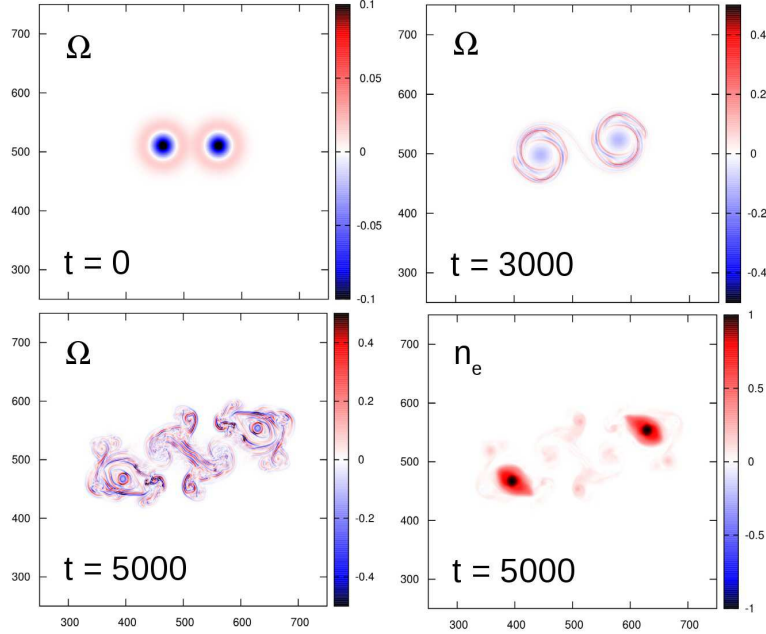


FIG. 4: Explosive vortex repulsion out of two neighbouring “adiabatic blobs” with initial Gaussian density and potential perturbations with $n_e(\mathbf{x}, t_0) = \phi(\mathbf{x}, t_0)$, which results in a shielded initial vorticity. Ω is shown at three times, and density n_e also at $t = 5000 \omega_i^{-1}$.

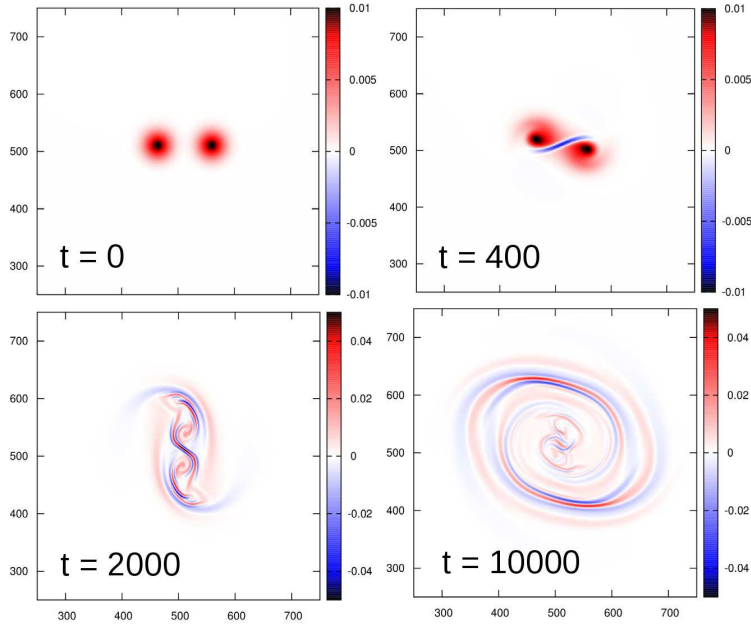


FIG. 5: FLR accelerated merging for “adiabatically” ($n_e(\mathbf{x}, t_0) = \phi(\mathbf{x}, t_0)$) initialised Gaussian vorticity.

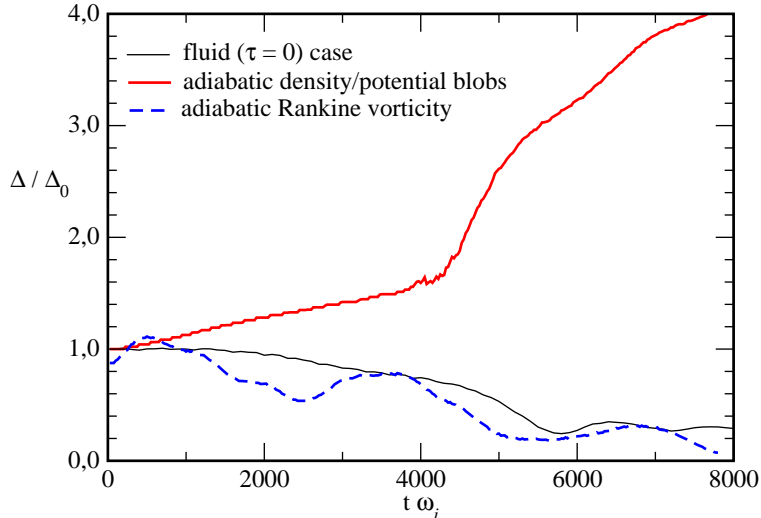


FIG. 6: Explosive separation of “adiabatic blobs” (thick red curve). The “adiabatic Gaussian” case (dashed blue curve) shows again FLR induced acceleration of merging compared to the fluid-like (thin black curve) case.

The “adiabatic Gaussian” case is shown in Fig. 5: the development of vorticity is more similar to the fluid-like case (compare Fig. 1), but again with a pronounced FLR induced filamentary fine structure and accelerated merging. The evolution of peak separation Δ is for both “adiabatic” cases presented in Fig. 6. Both cases are again anti-symmetric after reversal of the initial amplitude.

From these examples it is obvious that the gyrofluid merger dynamics strongly depends on the initial vorticity and density distributions, in addition to parameters like initial relative vortex separation as in the fluid case.

VI. GYROSPINNING OF ASYMMETRIC VORTICES

A unique effect that is here present for all warm ion gyrofluid vortices is FLR induced spinning. A related FLR spin-up has been observed before for the special case of an interchange unstable (magnetic curvature driven) “blob”, which is characterised by the formation of a dipolar potential on top of a monopolar (e.g. Gaussian) density or pressure perturbation [19–21]. While interchange “blobs” can acquire spinning by a range of additional mechanisms [15, 22], the FLR spin-up is in the following shown to be a universal phenomenon and essentially a consequence of asymmetry. A single inviscid axially exactly symmetric vortex

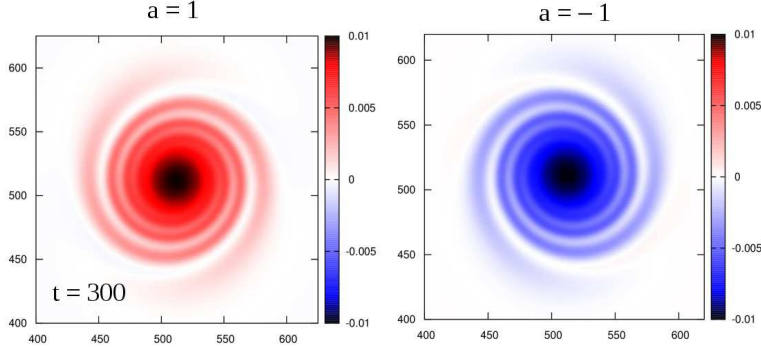


FIG. 7: *FLR spin-up of vorticity spiral arms in an asymmetric vortex with positive (left) and negative (right) initial elongated vorticity distribution $\Omega(\mathbf{x})$.*

retains its shape. In Fig. 7 the spin-up of FLR spiral arms is demonstrated for a single elongated vortex ($r_y = 1.2 r_x$), initialised by eqs. (5, 6) with $a = +1$ (left) and $a = -1$ (right).

From eq. (8) the FLR polarisation contribution to the evolution of vorticity is given as $d_t\Omega \sim \frac{\tau_i}{2}[\Omega, n]$. In polar (r, θ) coordinates centered on the vortex, $[\Omega, n] \sim (\partial_r\Omega)(\partial_\theta n) - (\partial_\theta\Omega)(\partial_r n)$ at a unit radius. For any axially symmetric $\Omega(\mathbf{x}) \sim n(\mathbf{x})$ the FLR polarisation vanishes.

For initial distributions close to Gaussian, $\partial_r \sim (1/\sigma)$ can be approximated. For symmetric $\Omega(t_0)$ but $n = n(\theta)$, as by elongation, with $\partial_\theta \sim ik_\theta$ a dispersion relation $\omega = (\tau_i/2\sigma)k_\theta \text{sgn}(B \cdot \Omega)$ is obtained. A spatial density asymmetry thus spreads vorticity azimuthally with $v_\theta \sim (\tau_i/2\sigma) \text{sgn}(B \cdot \Omega)$. Similarly, any radial density gradient from $n(r)$ leads to radial spreading of vorticity. The combined result is the spin-up of spiral arms as in Fig. 7 with orientation depending on the relative sign of magnetic field \mathbf{B} and vorticity Ω . Two neighbouring vortices mutually induce initial asymmetries similar to elongation, resulting in rapid pre-merging spin-up.

As a side remark, asymmetry can enter not only via non-circular vortex initialisation, but also numerically through a coarse rectangular grid and too close boundary proximity. Grid size and resolution have to be chosen accordingly, that any grid spin-up artefacts evolve much slower than the physical time scales of interest.

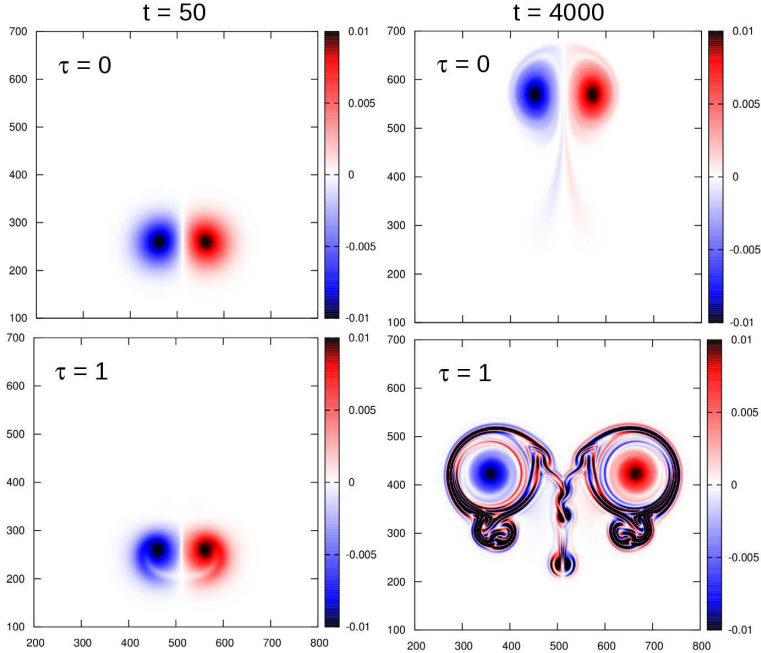


FIG. 8: Co-advection of counter-rotating vortices at two times for the fluid-like ($\tau_i = 0$) case (top row), and with FLR induced spin-up for $\tau_i = 1$ (bottom row).

VII. VORTICITY FILAMENTATION IN VORTEX CO-ADVECTION AND TURBULENCE

The complementary problem to merging of co-rotating 2D vortices is the straight co-advection of counter-rotating vortices. In Fig. 8 it is shown that FLR spin-up again significantly alters this type of vortex interaction: in a warm gyrofluid (bottom row) the vorticity filamentation slows the joint propagation but separates the vortex cores compared to the fluid-like cold case.

In combination, merging and co-advection determine the interactions and cascade in a turbulent sea of 2D vortices. We find that in decaying turbulence initialised with a random distribution of density and vorticity fluctuations analogously to eqs. (7, 8), the FLR induced spinning also leads to enhanced vorticity filamentation. Self-sustained drift-wave turbulence in inhomogeneous magnetised plasmas is in 2D effectively represented by the Hasegawa-Wakatani model [23]: the turbulent drive is maintained by a dissipative coupling term $d(\phi - n_e)$ added to the right hand side of eq. (2) for electrons, which emulates parallel electron dynamics for a single parallel wave number by the parameter d . A comparison of

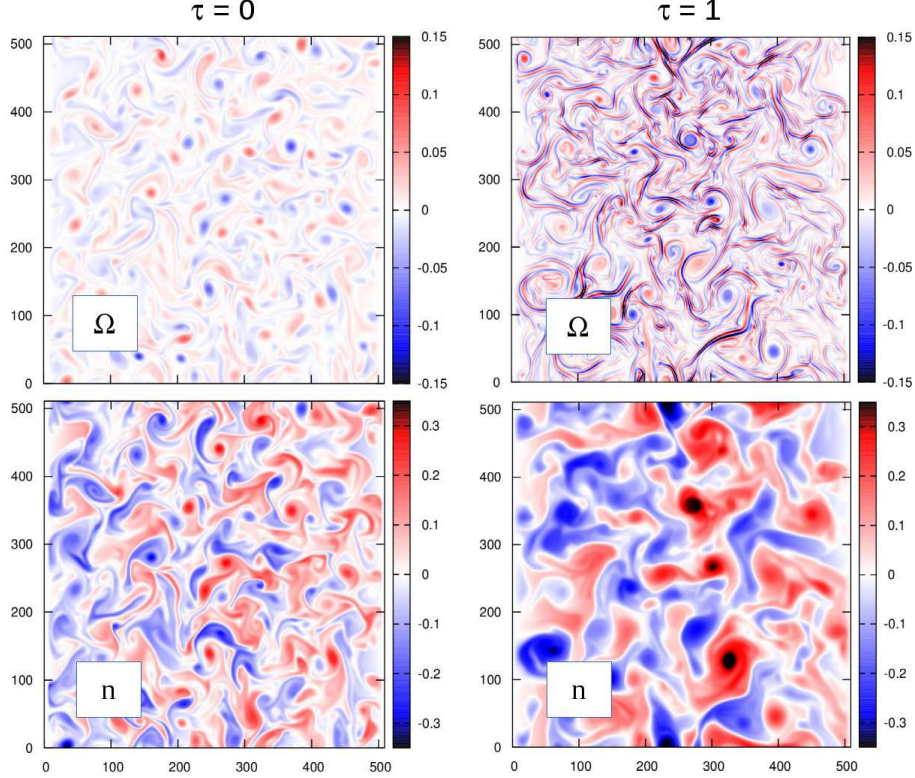


FIG. 9: Vorticity and density fields in fully developed cold and warm Hasegawa-Wakatani drift wave turbulence: $\Omega(\mathbf{x})$ shows FLR-induced filamentation, and density fluctuations $n(\mathbf{x})$ are enhanced on intermediate ($\rho_i k_\perp \sim 1$) scales.

the vorticity structure between $\tau_i = 0$ and 1 in a saturated drift wave turbulent state for $d = 0.01$ is shown in Fig. 9, and demonstrates the persistence of FLR induced vorticity filamentation in fully developed turbulence.

Vorticity thinning has been identified as a possible explanation for the inverse energy cascade of 2D turbulence in general fluids [24, 25] and for drift wave turbulence [26], and is here shown to be strongly enhanced by FLR spin-up in a gyrofluid. The amplitude of vorticity is for $\tau_i = 1$ increased over the whole spectral range, while density fluctuation amplitudes are enhanced on intermediate ($\rho_i k_\perp \sim 1$) scales.

In 3D warm gyrofluid computations of drift wave turbulence we find that the vorticity sheets are much less pronounced but still discernible. The parallel connection of fluctuations along the magnetic field lines in presence of radial zonal flow [28] and magnetic shear [27] distorts but not completely suppresses the filamentary spin-up.

VIII. CONCLUSIONS

In summary, vortex spiraling by gyroorbit effects has been shown to strongly impact all vortex interactions in quasi-2D magnetised plasma dynamics. The spin-up of spiral arms was explained by an effect of density asymmetries on the governing drift velocities through polarisation of gyroorbits. The nature and morphology of drift wave turbulence, which is of overall importance in magnetised fusion plasmas, is essentially changed. Gyrofluid (and gyrokinetic) simulations are able to consistently account for FLR effects on vorticity filamentation by sufficient spatial resolution.

Acknowledgements

The author thanks M. Held (Innsbruck) for valuable discussions.

This work was supported by the Austrian Science Fund (FWF) project Y398.

-
- [1] R.H. Kraichnan and D. Montgomery, *Rep. Prog. Phys.* **43**, 547 (1980).
 - [2] G. Boffetta and R.E. Ecke, R.E., *Annu. Rev. Fluid Mech* **44**, 427 (2012).
 - [3] W. Horton and A. Hasegawa, *Chaos* **4**, 227 (1994).
 - [4] W. Horton, *Rev. Mod. Phys.* **71**, 735 (1999).
 - [5] B.D. Scott, A. Kendl, T. Ribeiro, *Contrib. Plasma Phys.* **50**, 228 (2010).
 - [6] T.S. Hahm, *Phys. Fluids* **31**, 2670 (1988).
 - [7] Brizard A.J. & Hahm, T.S. Foundations of nonlinear gyrokinetic theory. *Rev. Mod. Phys.* **79**, 421 (2007).
 - [8] Krommes, J.A. The gyrokinetic description of microturbulence in magnetized plasmas. *Annu. Rev. Fluid Mech.* **44**, 175 (2012).
 - [9] G. Knorr, et al., *Physica Scripta* **38**, 829 (1988)
 - [10] W. Dorland and G. Hammett, *Phys. Fluids B* **5**, 812 (1993).
 - [11] M.A. Beer and G.W. Hammett, *Phys. Plasmas* **3**, 4046 (1996).
 - [12] B. Scott, *Phys. Plasmas* **12**, 102307 (2005).
 - [13] B. Scott, *Plasma Phys. Control. Fusion* **45**, A385 (2003).

- [14] B. Scott, *Phys. Plasmas* **17**, 102306 (2010).
- [15] A. Kendl, *Plasma Phys. Control. Fusion* **57**, 045012 (2015).
- [16] D. Pfirsch, *Z. Naturforsch.* **39a**, 1 (1984).
- [17] A.J. Brizard, *Phys. Plasmas* **20**, 092309 (2013).
- [18] T. Leweke, S. Le Dizes, and C.H.K. Williamson, *Annu. Rev. Fluid Mech* **48**, 507 (2016).
- [19] J. Madsen, et al., *Phys. Plasmas* **18**, 112504 (2011).
- [20] M. Wiesenberger, J. Madsen, A. Kendl, *Phys. Plasmas* **21**, 092391 (2014).
- [21] M. Held, M. Wiesenberger, J. Madsen, A. Kendl, *Nucl. Fusion* **56** 126005 (2016).
- [22] D.A. D'Ippolito, J.R. Myra, D.A. Russell, G.Q. Yu, *Phys. Plasmas* **11**, 4603 (2004).
- [23] A. Hasegawa, A. and M. Wakatani, *Phys. Plasmas* **14**, 102312 (2007).
- [24] S. Chen, et al., *Phys. Rev. Lett.* **96** 084502 (2006).
- [25] C.H. Bruneau, P. Fischer, H. Kellay, *Europhysics Letters* **78**, 34002 (2007)
- [26] P. Manz, G. Birkenmeier, M. Ramisch, U. Stroth, *Phys. Plasmas* **19**, 082318 (2012).
- [27] A. Kendl, and B.D. Scott, *Phys. Rev. Lett.* **90**, 035006 (2003).
- [28] Z. Lin, T.S. Hahm, W.W. Lee, W.M. Tang, R.B. White, *Science* **281**, 1835 (1998).